

## Multicomponent Polymer Brushes

Feng Zhou,<sup>†</sup> Zijian Zheng,<sup>†</sup> Bo Yu,<sup>‡</sup> Weimin Liu,<sup>‡</sup> and Wilhelm T. S. Huck<sup>\*,†</sup>

Contribution from the State Key Laboratory of Solid Lubrication, Lanzhou Institute of Chemical Physics, Chinese Academy of Sciences, Lanzhou 730000, P.R. China, and Melville Laboratory for Polymer Synthesis, University of Cambridge, Lensfield Road, Cambridge CB2 1EW, U.K.

Received July 28, 2006; E-mail: wtsh2@cam.ac.uk

**Abstract:** This article describes a general synthetic route to laterally distinctive multicomponent polymer brushes on gold. The procedure involves repeated surface patterning using microcontact printing ( $\mu$ CP) of initiator-terminated thiols without backfilling with inert thiols and surface-initiated atomic transfer radical polymerization steps. In between brush growth, the remaining initiator moieties are deactivated to avoid reinitiation on existing brushes. Optical and fluorescence microscopy, atomic force microscopy, attenuated total reflectance Fourier transform infrared spectroscopy, and X-ray photoelectron spectroscopy have been used to characterize every step of this procedure. We found that brushes can be grown from initiator-modified surfaces that contain bare gold areas and that these areas remain available for further patterning using  $\mu$ CP. To demonstrate the flexibility of this approach, surfaces containing four different polymer brushes in patterns ranging from  $2 \times 4 \mu\text{m}$  lines to  $20 \times 20 \mu\text{m}$  squares were fabricated. The range of chemical functionalities incorporated includes cationic and anionic polyelectrolytes, as well as thermally responsive polymers.

## Introduction

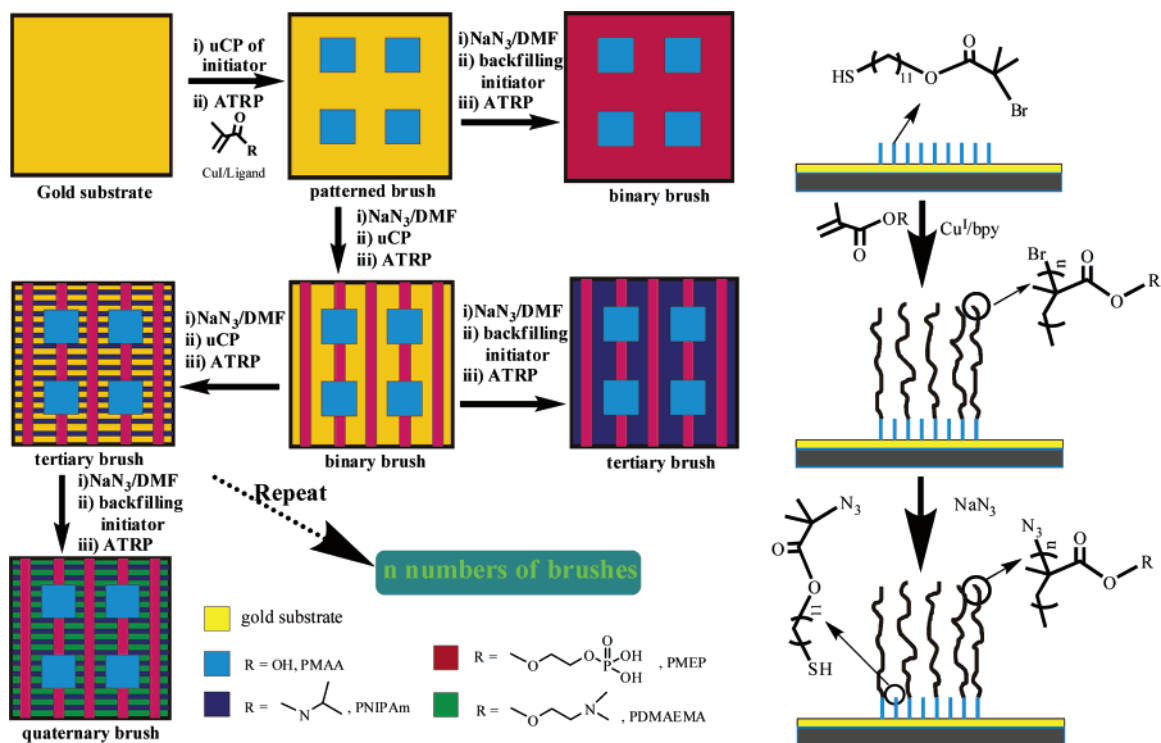
Polymer brushes have emerged as a robust method for creating surfaces with a wide range of mechanical and chemical properties and could in many ways act as ideal alternatives to self-assembled monolayers.<sup>1–6</sup> The use of polymers as building blocks for surface modification introduces the possibility to make a “smart” or responsive surface based on conformational changes in the polymer backbones. In recent years, a range of controlled surface-initiated polymerization techniques have been developed, allowing the formation of (block co-) polymer brushes with controlled grafting densities and thicknesses.<sup>7–9</sup> Patterned polymer brushes are routinely produced by patterning the initiator monolayer.<sup>10–13</sup> However, only a limited number of routes to laterally patterned binary polymer brushes (i.e., two

polymers next to each other) have been reported: (i) Kang and co-workers have used self-assembled monolayers containing patterns of two different initiators, followed by sequential, orthogonal polymerization steps,<sup>14</sup> (ii) R uhe and co-workers used photoinitiated free-radical polymerization from successively irradiated areas,<sup>15</sup> (iii) Zhou et al.<sup>16</sup> prepared binary brushes via photoetching and reinitiation, and (iv) Luzinov<sup>17</sup> recently reported the use of an imprinted masking layer to form binary brushes. All these methods involved complex lithographic schemes, which are difficult to implement when using sensitive polymers and cannot be taken beyond the formation of binary brushes (i.e., surfaces containing two different polymers). In this article, we present a generic, purely additive approach to the formation of four component brushes, and we believe that this new route could be further extended with any number of polymers, enabling the “synthesis” of very complex polymer surfaces. Such surfaces could find use as model substrates for tissue engineering or biosensors, where very often a complex range of chemical functionalities in a well-defined spatial arrangement are required. Surfaces containing multiple responsive polymer brushes could also be used for guided flow in microfluidic devices and for tuning surface roughness at different length scales. It is interesting to note that despite the enormous activity in the area of patterned SAMs, very few strategies have been developed for patterning surfaces with an arbitrary number

<sup>†</sup> University of Cambridge.<sup>‡</sup> Chinese Academy of Sciences.

- (1) Advincula, R. C.; Brittain, W. J.; Caster, K. C.; Ruehe, J. *Polymer Brushes: Synthesis, Characterization, Applications*; Wiley-VCH: Weinheim, Germany, 2004.
- (2) Senaratne, W.; Andruzzi, L.; Ober, C. K. *Biomacromolecules* **2005**, *6*, 2427.
- (3) Zhou, F.; Huck, W. T. S. *Phys. Chem. Chem. Phys.* **2006**, *8*, 3815.
- (4) Jennings, G. K.; Brantley, E. L. *Adv. Mater.* **2004**, *16*, 1983.
- (5) Tomlinson, M. R.; Genzer, J. *Chem. Commun.* **2003**, 1350.
- (6) Dyer, D. J. *Adv. Funct. Mater.* **2003**, *13*, 667.
- (7) Edmondson, S.; Osborne, V. L.; Huck, W. T. S. *Chem. Soc. Rev.* **2004**, *33*, 14.
- (8) Lee, W.-K.; Kaholek, M.; Ahn, S. J.; Zauscher, S. Nanopatterning of Stimulus-Responsive Polymer Brushes by Scanning Probe and Electron Beam Lithography. In *Responsive Polymer Materials: Design and Applications*; Minko, S., Ed.; Blackwell Publishing: Oxford, U.K., 2006; p 84.
- (9) Brittain, W. J.; Boyes, S. G.; Granville, A. M.; Baum, M.; Mirous, M. K.; Akgun, B.; Zhao, B.; Blickle, C.; Foster, M. D. *Adv. Polym. Sci.* **2006**, *198*, 125.
- (10) Husemann, M.; Mecerreyes, D.; Hawker, C. J.; Hedrick, J. L.; Shah, R.; Abbott, N. L. *Angew. Chem., Int. Ed.* **1999**, *38*, 647.
- (11) Schmelmer, U.; Jordan, R.; Geyer, W.; Eck, W.; Golzhauser, A.; Grunze, M.; Ulman, A. *Angew. Chem., Int. Ed.* **2003**, *42*, 559.
- (12) Maeng, I. S.; Park, J. W. *Langmuir* **2003**, *19*, 4519.

- (13) Kaholek, M.; Lee, W. K.; Ahn, S. J.; Ma, H.; Caster, K. C.; Zauscher, S. *Nano Lett.* **2004**, *4*, 373.
- (14) Xu, F. J.; Song, Y.; Cheng, Z. P.; Zhu, X. L.; Zhu, C. X.; Kang, E. T.; Neoh, K. G. *Macromolecules* **2005**, *38*, 6254.
- (15) Prucker, O.; Habicht, J.; Park, I. J.; R uhe, J. *Mater. Sci. Eng., C* **1999**, *8*, 291.
- (16) Zhou, F.; Jiang, L.; Liu, W. M.; Xue, Q. *Macromol. Rapid Commun.* **2004**, *25*, 1979.
- (17) Liu, Y.; Klep, V.; Luzinov, I. *J. Am. Chem. Soc.* **2006**, *128*, 8106.

**Scheme 1.** Outline Procedure for Grafting Multiple Patterned Polymer Brushes and ATRP Passivation

of different alkylthiols or silanes.<sup>18,19</sup> It might well be that the design rules for patterned polymer brushes, where imperfections at the molecular level are easily “repaired” due to relaxation of the stretched polymer chains, are less stringent than that for their small-molecule counterparts.

The experimental procedure followed in this work is summarized in Scheme 1. First, a patterned, initiator-terminated thiol monolayer (with a bare gold background) prepared by microcontact printing ( $\mu\text{CP}$ ) is used in a surface-initiated polymerization step using atom transfer radical polymerization (ATRP).<sup>20</sup> Subsequently, the “living” chain end is passivated via a nucleophilic substitution reaction with  $\text{NaN}_3$ . The next initiator SAM is then contact-printed onto the surface, and the second brush is grown in those areas that were in contact with the stamp and had not previously been modified with a polymer brush. After passivation, a third set of brushes can be grown upon printing another initiator SAM. Finally, backfilling the unmodified areas results, after  $n$  printing steps, in the formation of brushes in the background. One can stop printing at any time by backfilling with initiator and performing the final polymerization step.

## Experimental Section

**Chemicals.** General chemicals were analytical reagent grade and were used as received from Sigma Aldrich, Fisher, or Lancaster. Methacrylic acid sodium (MAA-Na), methacryloylolethylphosphate (MEP), *N*-isopropylacrylamide (NIPAM), and *N,N'*-dimethylamino ethyl methacrylate (DMAEMA) were obtained from Aldrich. Milli-Q water was generated with a Millipore Simplicity 185 system. Inhibitors in the monomers were removed by elution through a neutral alumina plug before use. Copper(I) bromide ( $\text{CuBr}$ ), 2,2'-dipyridyl (99%) (bpy), and

pentamethyldiethylenetriamine (PMDETA) were all obtained from Aldrich. Gold film was prepared via thermo evaporation of 200-nm gold on silicon wafers (Compart Technology Ltd., 100-mm diameter, boron-doped, (100) orientation, one side polished) with 2-nm Cr as the adhesive layer. Acridine orange base was purchased from Aldrich.

**Characterization.** AFM experiments were carried on a MAC Mode Pico-SPM magnetically driven dynamic force microscope (Molecular Imaging). AFM data was processed with WSxM software (Nanotec Electrónica). Optical and fluorescent images were taken with a Nikon microscope (ECLIPSE ME600L) equipped with a Y-FL Epi-fluorescence attachment. Attenuated total reflectance Fourier transform infrared (ATR-FTIR) spectra were obtained on a Perkin-Elmer Spectra One spectrometer with Universal ATR accessory. X-ray photoelectron spectra were obtained on a PHI-5702 multifunctional X-ray photoelectron spectroscope (XPS) at a takeoff angle of  $45^\circ$  and with a resolution of  $\pm 0.2$  eV, using the Mg  $K\alpha$  irradiation as the excitation source and the binding energy of C1s at 284.6 eV as reference.

**Surface-Initiated Polymerizations.**  $\omega$ -Mercaptoundecyl bromoisobutyrate was synthesized following a published procedure.<sup>21</sup> The general polymerization procedure involved dissolving the monomer in water or water/methanol mixed solvent at room temperature and degassing by passing a continuous stream of dry  $\text{N}_2$  through the solution while being stirred (30 min). To this solution were added bpy or PMDETA, and  $\text{CuBr}$  successively. The mixture was then further stirred and degassed with a stream of dry  $\text{N}_2$  until a clear solution formed. For microcontact printing, 5 mM initiator solution was spread onto the PDMS stamp, was blow dried, and made contact with gold surface for 20 s.  $\mu\text{CP}$  on surfaces already patterned brushes was carried out in a similar way, with slight pressing to ensure conformal contact. Initiator-patterned gold substrates were sealed in Schlenk tubes and degassed (four times high-vacuum pump/ $\text{N}_2$  refill cycles). Polymerization solutions were injected into a Schlenk tube for reaction for a certain time. Polymerization recipes for the four monomers are as following: MAA-Na 9 g,  $\text{CuBr}$  0.288 g, bpy 0.62 g, 27 mL of water,  $60^\circ\text{C}$ , 30 min.<sup>22</sup> MEP 31.5 g was neutralized with 10 mol/L NaOH to pH 7, and

(18) Wilbur, J. L.; Biebuyck, H. A.; MacDonald, J. C.; Whitesides, G. M. *Langmuir* **1995**, *11*, 825.

(19) Dameron, A. A.; Hampton, J. R.; Gillmor, J. R.; Hohman, J. N.; Weiss, P. S. *J. Vac. Sci. Technol., B* **2005**, *23*, 2929.

(20) Jones, D. M.; Huck, W. T. S. *Adv. Mater.* **2001**, *13*, 1256.

(21) Jones, D. M.; Brown, A. A.; Huck, W. T. S. *Langmuir* **2002**, *18*, 1265.

(22) Zhou, F.; Huck, W. T. S. *Chem. Commun.* **2005**, 5999.

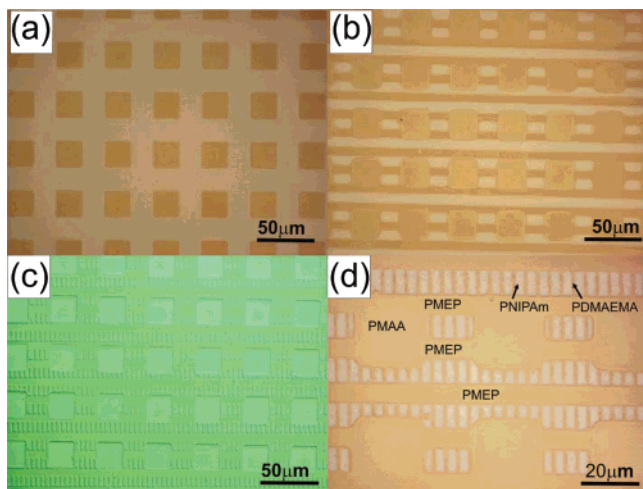


**Figure 1.** Evolution of optical microscopic images of patterned polymer brushes following the fabrication process shown in Scheme 1. (a) First brush PMAA ( $20 \times 20 \mu\text{m}$  square), (b) after grafting the second brush, PMEP ( $5 \times 10 \mu\text{m}$  lines), (c) after grafting the third brush, PNIPAm (crossed  $2 \times 4 \mu\text{m}$  lines perpendicular to  $5 \times 10 \mu\text{m}$  lines), and (d) after grafting the fourth brush PDMAEMA (in backfilled areas).

the volume was adjusted to 50 mL. bipy 0.312 g, CuBr 0.144 g,  $60^\circ\text{C}$ , 30 min.<sup>23</sup> NIPAm 12.6 g, CuBr 0.16 g, PMDETA 0.581 g, water/methanol (12.6 mL, 1/1 v/v), 30 min.<sup>24</sup> DMAEMA 15.7 g, CuBr 0.288 g, bpy 0.62 g, water/methanol (30 mL, 1/1 v/v), 1 h. Passivation of the polymer brushes was carried out by reacting in 0.1 M  $\text{NaN}_3/\text{DMF}$  solution at  $50^\circ\text{C}$  for more than 6 h, followed by rinsing with DMF and water.

## Results and Discussion

To prepare quaternary brushes (i.e., surfaces containing four different polymer brushes), we used a  $20\text{-}\mu\text{m}$  square stamp to grow the first brushes (PMAA),  $5 \times 10 \mu\text{m}$  lines for the second brushes (PMEP),  $2 \times 4 \mu\text{m}$  lines printed at a  $90^\circ$  angle for the third brushes (PNIPAm),<sup>25</sup> and backfilling with PDMAEMA brushes. Figure 1 shows the brush-patterned surfaces after the respective printing and brush growth steps, and it is clear that our procedure yields multicomponent brushes in complex patterns, all of which are well-defined. These images also provide a first indication that no brushes regrow from areas previously patterned with brushes (as this would lead to contrast difference within, for example, the  $20\text{-}\mu\text{m}$  squares). We also used AFM to measure the thickness of each brush after printing and surface-initiated polymerization. The thicknesses for the different brushes shown in Figure 1d are PMAA 20 nm, PMEP 30 nm, PNIPAm 75 nm, and PDMAEMA 30 nm. Figure 2 shows optical and fluorescence microscopy images of a different set of multicomponent brushes. In Figure 2a, PMAA/PDMAEMA binary brushes patterned into  $5 \times 10 \mu\text{m}$  lines were obtained with one printing and backfilling cycle. The polymer brushes were then stained (Figure 2b) with a cationic fluorescent dye, acridine orange base, which is well-known to exhibit pH-dependent fluorescence colors.<sup>26,27</sup> The red fluorescence observed here strongly indicated accumulation inside anionic brushes and

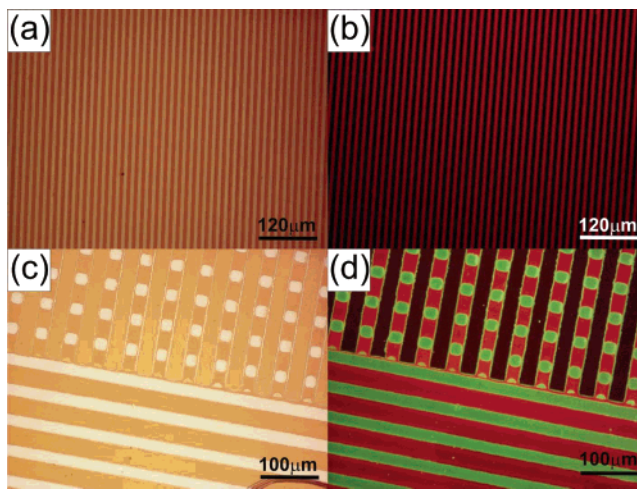


**Figure 2.** (a) Optical microscopic image of acridine-stained PMAA/PDMAEMA binary brush (the dark area is PMAA) and (b) the corresponding fluorescence image (the bright red area is PMAA). (c) Tertiary brush of acridine-stained PMAA/PMEP/PNIPAm and (d) the corresponding fluorescence image (bright red area is PMEP; the green area is PNIPAm).

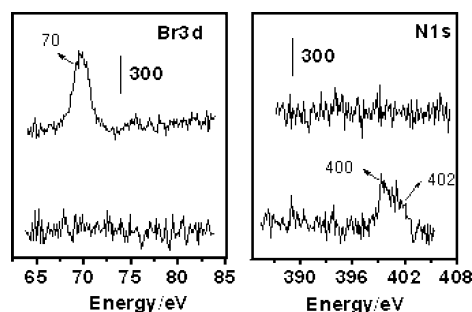


**Figure 3.** XPS of Br3d and N1s regions before (top trace) and after (bottom trace) reaction with 0.1 M  $\text{NaN}_3/\text{DMF}$  for 6 h.

PMAA brushes. Tertiary brushes were prepared by printing  $25 \times 25 \mu\text{m}$  lines twice,  $90^\circ$  to each other, growing lines of PMAA and PMEP brushes, with PNIPAm filled into the background.<sup>13</sup> Figure 2c,d shows optical and fluorescence microscopy images of acridine orange stained multicomponent brushes. The dark area in Figure 2d is PMAA, and the bright red area is PMEP; the contrast is due to their different affinity for the acridine base. The green areas are the PNIPAm brushes, and the difference in color is due to the different chemical environment provided by the PNIPAm versus the PMEP brushes.

Some concerns need to be addressed to ensure the success of the approach described above. Previously, patterned polymer brushes were grown from patterned initiator SAMs backfilled with an inert thiol to avoid any spreading of the initiator thiols. Serendipitously, we found that omitting the backfilling step did not result in any obvious initiator diffusion, nor in physisorption of polymers in the bare Au areas, and control experiments showed identical patterns when using backfilled and non-backfilled patterns (data not shown). This is a key breakthrough in allowing the buildup of chemically more complex patterns. Another important issue is the risk of reinitiation from previously grown brushes. ATRP is a controlled radical polymerization,<sup>28</sup> and therefore the halogen initiator moieties at the end of the polymer chains and also any nonreacted initiator monolayer underneath the brushes need to be “terminated” to avoid growth

(23) Osborne, V. L.; Jones, D. M.; Huck, W. T. S. *Chem. Commun.* **2002**, 1838.

(24) Jones, D. M.; Smith, J. R.; Huck, W. T. S.; Alexander, C. *Adv. Mater.* **2002**, *14*, 1130.

(25) Li, H.-W.; Muir, B. V. O.; Fichet, G.; Huck, W. T. S. *Langmuir* **2003**, *19*, 1963.

(26) Shimosaka, T.; Sugii, T.; Hobo, T.; Ross, A. J. B.; Uchiyama, K. *Anal. Chem.* **2000**, *72*, 3532.

(27) Clerc, S.; Barenholz, Y. *Anal. Biochem.* **1998**, *259*, 104.

(28) Matyjaszewski, K.; Xia, J. *Chem. Rev.* **2001**, *101*, 2921.

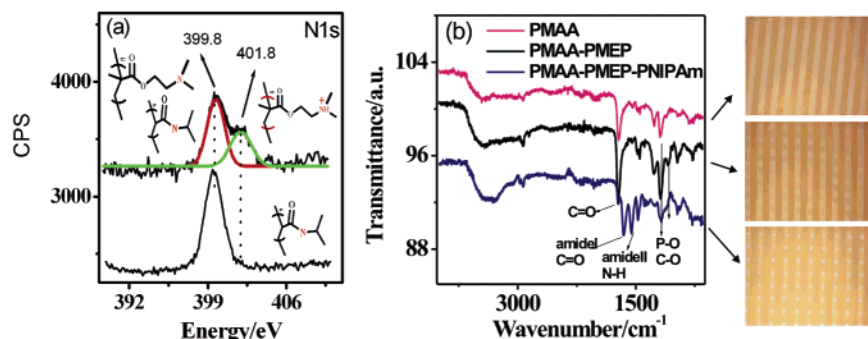


**Figure 4.** (a) XPS spectra of multicomponent brushes showing changes in the N1s peak region upon backfilling PMAA/PMEP/PNIPAm (bottom trace) with PDMAEMA (top trace). (b) ATR-FTIR and optical images of patterned, binary, and tertiary polymer brushes.

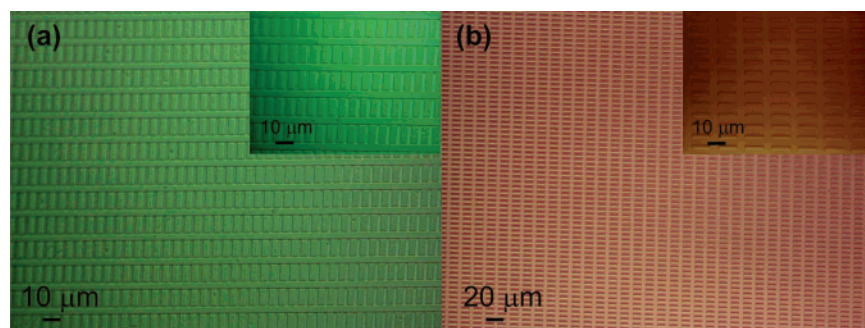


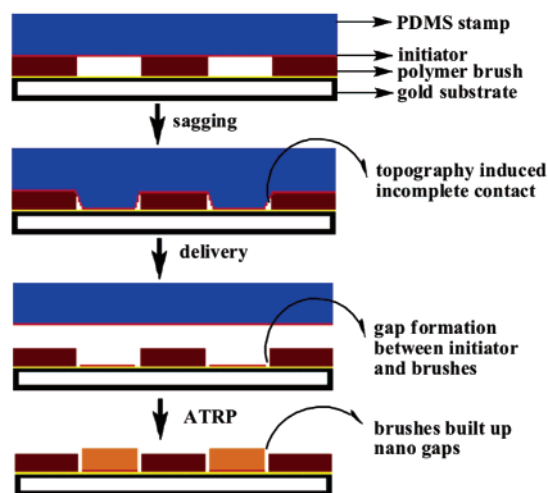
**Figure 5.** (a) Binary PNIPAM brushes, with the second initiator SAM printed after growth of a 15-nm-thick PNIPAM brush. (b) Cross-printed initiator SAMs before any brush growth.

of copolymer or mixed brushes. We therefore carried out a nucleophilic substitution reaction with  $\text{NaN}_3$  to passivate the reactive sites.<sup>16,29</sup> XPS experiments on initiator SAMs verified the transformation of a terminal halogen functionality to azides. Figure 3 shows that after the reaction the Br 3d peak at 70 eV disappeared, concomitant with the appearance of an N1s peak as two partly overlapped peaks at 400 and 402 eV, which is attributable to the two different N atoms in the azide group. When these SAMs were used as substrates for brush growth, no increase in thickness was observed; similarly, polymer brushes treated with  $\text{NaN}_3$  could not be reinitiated.

Multicomponent brushes were further characterized using XPS, ATR-FTIR, and AFM. XPS was used to verify the growth of PDMAEMA brushes, backfilled in between tertiary PMAA/PMEP/PNIPAm brushes. As shown in Figure 4a, the XPS spectrum shows a single N1s peak at 399.8 eV, attributable to nitrogen in PNIPAm having a single chemical environment. After grafting PDMAEMA, an N1s peak at 401.8 eV appears as a shoulder, which is attributed to the protonated nitrogen in the tertiary amine. Figure 3b shows FTIR spectra and the corresponding optical images of the buildup of a tertiary brush surface containing PMAA, PMEPE, and PNIPAm brushes via two orthogonal printing steps followed by a final backfilling with PNIPAm brushes. Despite the increasing complexity of the spectra and the overlap between signals of the different polymers, the introduction of the PNIPAm in the final step is clearly illustrated in the appearance of the amide I and amide II peaks.

Two undesirable possibilities might arise during  $\mu\text{CP}$  of initiator SAMs on top of brush patterned surfaces: (a) pattern transfer around the edges of brushes might be incomplete due

**Scheme 2.** Illustration of (Nano)gap Formation Due to Incomplete Stamp Contact



to incomplete stamp contact in these areas<sup>30</sup> and (b) initiator molecules might adhere to or become embedded in the polymer brushes. To illustrate that incomplete stamp contact can be a problem, we compared a binary brush pattern to a patterned surface that was prepared via cross-printing the initiator molecules (but without growing the brushes in between the printing steps). The left image in Figure 5 shows the appearance of a thin line when the second initiator SAM is printed after the growth of 15-nm thick PNIPAM brushes in the first cycle, whereas the right image in Figure 5, where the monolayers are printed in two steps, shows no such gap.

The formation of (nanoscale) gaps between the printed brushes is schematically explained in Scheme 2. After the first

(29) Coessens, V.; Pintauer, T.; Matyjaszewski, K. *Prog. Polym. Sci.* **2001**, *26*, 337.

(30) Zheng, Z.; Azzaroni, O.; Zhou, F.; Huck, W. T. S. *J. Am. Chem. Soc.* **2006**, *128*, 7730.

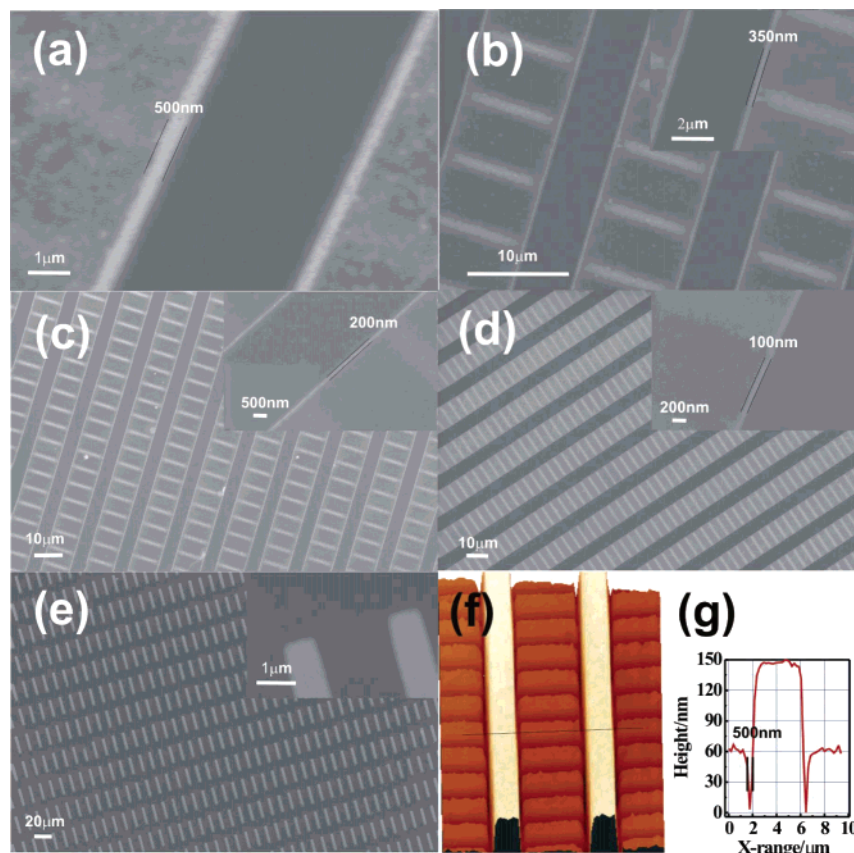


**Figure 6.** SEM images of binary (all PNIPAM) brushes showing gaps between the brushes due to incomplete contact of stamps. The initial brushes are (a) 150-, (b) 70-, (c) 45-, and (d) 15-nm thick. (e) Brushes grown from patterned SAMs. (f) AFM image of brushes 150-nm-thick initial brushes, with (g) line trace showing smooth brush surface.

patterned brush has been passivated, the stamp is placed on a topographically structured surface. As the height of the brushes is rather low, the stamp deforms and still forms good contact with the bare gold surface. However, close to the edge of the patterned brushes, this contact is lost and no new initiator SAM is transferred, resulting in a gap between adjacent brushes. This gap will eventually be filled with the brushes grown in the final backfilling step.

A more detailed study on a range of brushes with different heights revealed that, in all cases where we allowed the stamp to come in conformal contact with the surface without applying additional pressure, a small gap remained around the edges of the brushes (when the stamp is pressed firmly against the surface, the gap apparently disappears, but the printed features are distorted; results not shown). Figure 6 shows a range of SEM images that show a general trend of wider gaps with increasing thickness of the first brush. By varying the brush thickness between 15 and 150 nm, the gap due to incomplete stamp contact can be varied between 100 and 500 nm. It should be stressed that these values do depend strongly on the pressure applied to the stamps (as illustrated in Scheme 2), and at present the occurrence of these gaps is not sufficiently controlled to enable some sort of nanolithographic technique. Figure 6e shows an SEM image of brushes grown on a patterned SAM (prepared via two orthogonal prints), and clearly no gap is observed here.

It should be noted that the top surface of the initially printed brushes is in all cases very smooth, and we have found no evidence for any initiator molecules transferred to the brushes

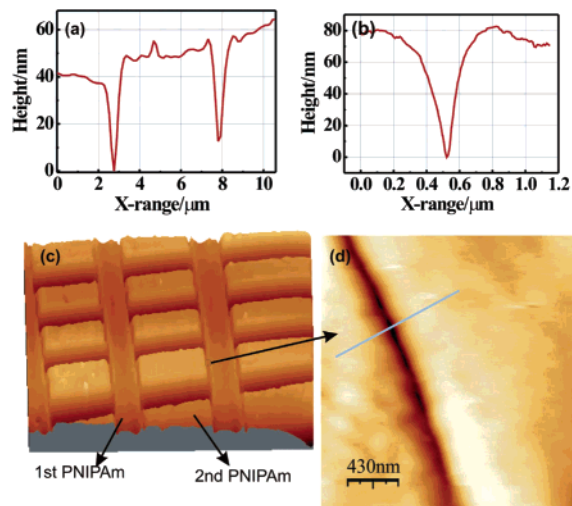


**Figure 7.** (a) Profile of binary PNIPAm (both are about 80 nm) in dry form showing gap. (b) Profile of gap in the swollen brushes under solution in (d). (c, d) AFM images of swollen binary PNIPAm in water.

leading to growth from those regions already carrying polymer brushes. Figure 7 shows another sample with again very clean polymer brush surfaces. It is clear that even when the second brush is grown to almost the same as the first brush (80 nm, see line trace in Figure 7a) the gap remains around 400 nm. The bottom set of AFM images in Figure 7c,d shows the same brushes under water and the gap remains clearly visible, although there seems to be some reduction in the width to around 300 nm (Figure 7b).

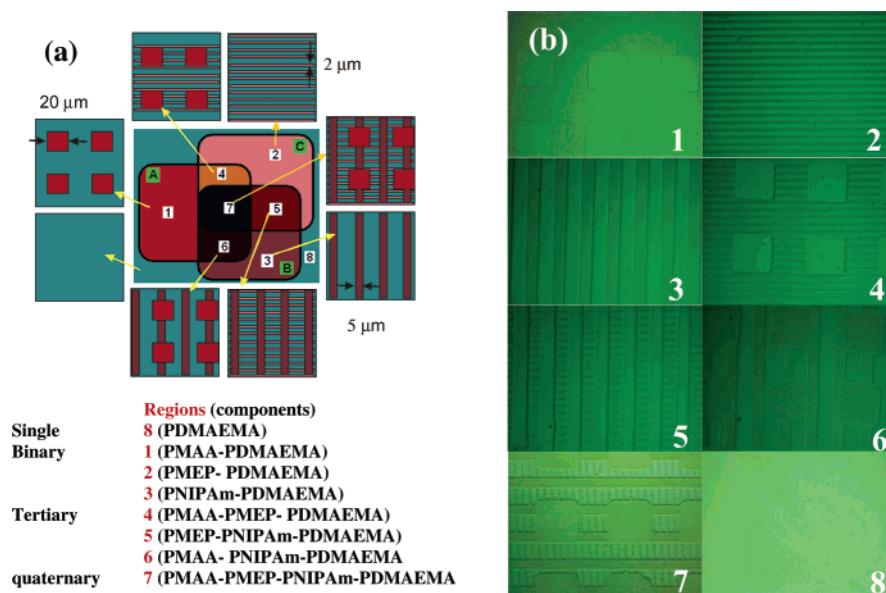


**Figure 8.** (a) Overview of different regions (1–8) obtained on the surface after three partially overlapping printing steps (A, B, and C) and four brush growth cycles (PMAA/PMEP/PNIPAm/PDMAEMA). (b) Images taken from different areas of a single surface shown in Figure 8a.

The versatility and ease of the  $\mu$ CP procedure enable the formation of very complex surfaces with various brush combinations that can be obtained in one polymerization sequence by allowing the printing steps to overlap partially. This idea is schematically represented in Figure 8a. For example, in a sequence with three partially overlapping  $\mu$ CP steps and a final backfilling step to yield quaternary brushes, the resulting surfaces contain up to eight different areas with different brush combinations. Figure 8b shows the optical images of different areas on such a surface consisting of a PMAA/PMEP/PNIPAm/PDMAEMA polymerization sequence. From these images, one can clearly see that such a patterning sequence leads to surfaces that contain all combinations of different polymers on one surface, which would enable studies where the influence of different surface chemistries on, for example, protein fouling of surfaces can be studied under well-controlled circumstances.

In conclusion, we have demonstrated a simple and soft lithographic approach to make laterally distinctive multicomponent polymer brushes. The method is based on our discovery that backfilling microcontact printed SAMs before brush growth is not necessary and that the remaining bare gold surface does

not need to be protected with a SAM during brush growth. In the present study, the polymers have been selected to show the versatility of our method to incorporate polymers with a range of functional groups, including cationic, anionic, and neutral polymers. In principle, our strategy can be extended to create surfaces with any number of brushes, but this will require a careful choice of PDMS stamps. Stamps with small feature sizes and large spacings will be preferable because large areas of bare gold can be left after one printing and grafting cycle. The small gaps observed between printed brushes could provide a new route to maskless nanopatterning of (sub-) 100-nm features, and new developments in printing technology<sup>31</sup> could aid in controlling this process, which is obviously dependent on contact time, pressure, and inking of the stamps.

**Acknowledgment.** We thank EPSPC (GR/T11555/01) and NSFC (50421502) and “973” project (2007CB607600) for financial support.

JA0654377

(31) Helmuth, J. A.; Schmid, H.; Stutz, R.; Stemmer, A.; Wolf, H. *J. Am. Chem. Soc.* **2006**, *128*, 9296.